plant biology

Plant Biology ISSN 1435-8603

RESEARCH ARTICLE

Role of cell wall polysaccharides in water distribution during seed imbibition of *Hymenaea courbaril* L.

A. Grandis[1,a], H. P. Santos[2,a], P. P. Tonini[1], I. S. Salles[1], A. S. C. Peres[3], N. C. Carpita[4] & M. S. Buckeridge[1]

1 Laboratório de Fisiologia Ecológica de Plantas, Lafieco -Departamento de Botânica, Instituto de Biociências, Universidade de São Paulo, São Paulo, Brazil
2 Centro Nacional de Pesquisa de Uva e Vinho, Bento Goncalves, Brazil
3 Instituto do Cérebro, Universidade Federal do Rio Grande do Norte. Av. Nascimento de Castro, Natal, Brazil
4 Biosciences Center, National Renewable Energy Laboratory, Golden, Colorado, USA

Keywords
arabinoxylan; cotyledons; germination; jatobá; Leguminosae; pectin; seed coat; xyloglucan.

Correspondence
M. S. Buckeridge, Laboratório de Fisiologia Ecológica de Plantas, Lafieco -Departamento de Botânica, Instituto de Biociências, Universidade de São Paulo, Rua do Matão, 277 CEP 05508-090, São Paulo, SP, Brazil.
E-mail: msbuck@usp.br

*These authors contributed equally to the work.

Editor
C. Seal

Received: 8 February 2024;
Accepted: 10 June 2024

doi:10.1111/plb.13688

ABSTRACT

- Seed water imbibition is critical to seedling establishment in tropical forests. The seeds of the neotropical tree *Hymenaea courbaril* have no oil reserves and have been used as a model to study storage cell wall polysaccharide (xyloglucan – XyG) mobilization.
- We studied pathways of water imbibition in *Hymenaea* seeds. To understand seed features, we performed carbohydrate analysis and scanning electron microscopy. We found that the seed coat comprises a palisade of lignified cells, below which are several cell layers with cell walls rich in pectin. The cotyledons are composed mainly of storage XyG. From a single point of scarification on the seed surface, we followed water imbibition pathways in the entire seed using fluorescent dye and NMRi spectroscopy. We constructed composites of cellulose with *Hymenaea* pectin or XyG. *In vitro* experiments demonstrated cell wall polymer capacity to imbibe water, with XyG imbibition much slower than the pectin-rich layer of the seed coat.
- We found that water rapidly crosses the lignified layer and reaches the pectin-rich palisade layer so that water rapidly surrounds the whole seed. Water travels very slowly in cotyledons (most of the seed mass) because it is imbibed in the XyG-rich storage walls. However, there are channels among the cotyledon cells through which water travels rapidly, so the primary cell walls containing pectins will retain water around each storage cell.
- The different seed tissue dynamic interactions between water and wall polysaccharides (pectins and XyG) are essential to determining water distribution and preparing the seed for germination.

INTRODUCTION

New plant individuals establish in different environments through dispersal, which depends on the physiological and biochemical characteristics of their seeds. Such establishment is restricted by storage reserves in the endosperm or cotyledons of seeds from the mother plant. Embryos and seedlings use storage reserves to sustain initial stages of growth until the seedling can obtain food from photosynthesis (Bewley & Black 1994).

The most distinct characteristic of angiosperms is the development of a seed encased in maternal tissue, called the seed coat (Volodymyr & Ljudmilla 2014). The seed coat is the primary barrier and defense against pathogens and pests, but also acts as a channel for transmitting environmental cues to the seed interior that trigger metabolism for germination after water diffusion (Egley 1989; Volodymyr & Ljudmilla 2014). Seeds have different strategies for water uptake control, and seed coats can be permeable or impermeable. Permeable seeds allow water entry, whereas impermeable seeds can block water entry for extended periods (Volodymyr & Ljudmilla 2014). 'Hardseededness' of impermeable seeds imposes coat-imposed dormancy (Bewley & Black 1994) or physical dormancy (Baskin *et al.* 2000) that enables seed survival in unfavorable environmental conditions (Rolston 1978; Tran & Cavanagh 1984). *Hymenaea courbaril* L. seeds exhibit such physical dormancy imposed by an impermeable seed coat that ensures longevity and viability even after long storage periods (Souza & Válio 2001).

Hymenaea courbaril L. (Leguminosae-Caesalpinioideae) is a semideciduous tropical tree family widely distributed across Neotropical regions of South America, from southern Brazil to Mexico (Lee & Langenheim 1975) (Figure S1). In Brazil, it is present in inventories of mature forests of eastern Amazonia and seasonal semideciduous forests (Schulze *et al.* 2008; Lopes *et al.* 2012). Mature *Hymenaea* trees generally occur at a low population density (<1 tree·ha^{-1}) and can reach a height of 45 and 3 m diameter at breast height (Carneiro *et al.* 2011). It is logged intensively in the Amazon region for high-density wood that is used for carpentry, furniture, and civil and naval construction (Lacerda *et al.* 2013), and also widely used in restoration projects in Brazil (Souza & Batista 2004; Sampaio

et al. 2007). This species also has medicinal and economic value for food, resin, and tannins (Martin *et al.* 1972; Stubblebine *et al.* 1978; Di Stasi *et al.* 2002). *Hymenaea* also has a high potential for carbon sequestration (Aidar *et al.* 2002).

The cotyledons of *Hymenaea* are rich in xyloglucans (XyG; 40% of seed dry mass), which is completely mobilized after germination (Tiné *et al.* 2000a). Storage XyG has a cellulose-like (1–4)-β-D-glucan backbone to which single (1–6)-α-D-xylopyranoside substituents are attached (Buckeridge *et al.* 2000b). Generally, xylosyl residues are regularly substituted at O-2 by β-D-galactopyranosyl residues (Hayashi 1989). The pattern of xylosyl substitution in XyG from *H. courbaril* is remarkably distinct from other seed XyG. Whereas nasturtium (*Tropaeolum majus*), tamarind (*Tamarindus indica*), and copaifera (*Copaifera langsdorffii*) XyG are composed of repetitive units of glucose-4:xylose-3 with variable galactosyl substitution (York *et al.* 1990; Buckeridge *et al.* 1992), *H. courbaril* XyG are composed of a mixture of glucose-4:xylose-3 and glucose-5:xylose-4 repetitive units with variable galactosyl substitutions (Buckeridge *et al.* 1997; Tiné *et al.* 2006; Buckeridge 2010; Buckeridge 2018). These differences in biochemical structure could impact imbibition and subsequent enzymatic degradation during germination (Buckeridge 2010). Seed storage XyG has a high molecular mass and low interaction with cellulose (Lima & Buckeridge 2001). However, these features may provide XyG with hydrodynamic packing properties that could impact water uptake by the seeds (Reid & Bewley 1979; Buckeridge *et al.* 1992; Buckeridge 2010).

Imbibition by seeds involves initial absorption of water, driven by the matric potential (a measure of the ability of a material to absorb water at its surface) of the cell walls. Initial water uptake can be localized, observed as a sharp wetting front along the seed coat, followed by more uniform hydration of the underlying cell walls (Vertucci & Leopold 1987). Concomitantly, a decrease in seed water potential is associated with an increase in seed water content (McDonald Jr *et al.* 1988a; Bradford 1990). Because water uptake occurs at the same rate in dead and living seeds, the entry rate into the seed depends on the matric potentials of the cell walls (Leopold 1980; Vertucci & Leopold 1983; Bewley & Black 1994). Paths of water flow in various seeds differ depending on the storage components, such as starch, lipids, and proteins in the cotyledons or endosperm (Buckeridge *et al.* 2000b; Nonogaki 2008; Yang *et al.* 2012). Some seeds, particularly those of legumes, have elaborated cell walls as a source of storage carbohydrates, usually XyG or galactomannan (Meier & Reid 1982; Buckeridge 2010).

Our study investigated how water travels through XyG-accumulating *Hymenaea* seeds from initial absorption by the seed coat to saturation of the cotyledon. Using ultrastructural analyses, we found that the *Hymenaea* seed coat resembles that typical of legume seeds, comprising an external layer of macro- and osteo-sclereides and a thick layer of cells rich in pectins and glucuronoarabinoxylans (GAX). Water first crosses the lignified layer in the external palisade of the seed coat before reaching an inner layer with pectin-rich cell walls, which facilitates rapid water absorption and dispersion. Swelling of the pectin gel matrix creates cracks, allowing water intake. While magnetic resonance imaging shows slow water distribution within the seed because of XyG, a network of intercellular channels swiftly distributes water through intercellular spaces in the cotyledons. *In vitro* testing of cellulose composites with XyGs and sead coat pectin confirmed the role of different individual polymers in seed water imbibition, establishing the unique physical properties crucial for *Hymenaea* seed germination.

MATERIAL AND METHODS

Plant description and sampling

Seeds of *Hymenaea* were collected from two trees growing in a gallery forest in São João da Boa Vista country, São Paulo, Brazil. In addition, we obtained seeds from trees of the same species and variety that were used for all chemical analyses at the University of São Paulo campus, Brazil. A total of 160 dry seeds (6–7% moisture content at harvest) were weighed, and mean seed mass was obtained. Seeds weighing 4.6–5.3 g (the median weight) were chosen for experiments. We dried the seeds in an oven at 100 °C to constant mass.

Proportional mass and imbibition of seed parts

Seed coats of 30 seeds were detached using a knife. The de-coated seeds were mechanically broken with a hammer to separate cotyledons and embryonic axes. These parts were dried at 70 °C for 72 h and weighed. Fifteen intact axes and pieces of similar shapes of seed coat and cotyledons were selected and distributed in a Petri dish containing filter paper moistened with water. Imbibition was followed at 20 °C. Every 2 h, seed parts were surface dried by paper blotting, weighed, and returned to the Petri dishes until they had all reached constant mass.

Imbibition

We scarified seeds with sandpaper in the lateral position to avoid damage to the embryo and removed only coat protection (<3 mm). Scarification was necessary due to the hard coat and water-impermeability of these seeds, which prevent prompt imbibition and germination under natural conditions (Souza & Válio 2001). Seeds only imbibed water in scarified regions in contact with the water. All experiments were performed at 25 °C. Every 24 h, 10 seeds were collected, surface blotted dry, weighed, and waterfront noted with the naked eye. To better visualize the water entering the seed coat and water distribution throughout the cotyledons, we used 0.5 $mg{\cdot}ml^{-1}$ Fluorescein sodium salt (Sigma-Aldrich-F6377) in water. Imbibition was followed in five scarified seeds as uptake of Fluorescein solution from a cotton bed. The scarified region remained in contact with the solution in darkness for up to 144 h at 25 °C. At intervals, transverse section images of the seeds (cut in half) were collected under brightfield and fluorescence imaging using a stereomicroscope, Leica M205 FA, lens 0.5×, with a GFP filter, excitation 470 nm, emission 525 nm. Images were processed using the Leica Application Suite software (LAS, version 4.8).

Nuclear magnetic resonance imaging (NMRI)

Seeds imbibed water from moistened filter paper for 24–144 h at 25 °C. The NMRI experiments used a Varian Inova, f 2.1

Tesla (85 MHz), equipped with an Oxford superconductor magnet with bore size 30 cm. The analyses were performed at Embrapa Instrumentation (São Carlos, São Paulo, Brazil). Seeds images were acquired using a spin-echo pulse sequence (Callaghan 1991) with an echo time of 30 ms; the seeds were sliced to 0.5 cm thickness, and images were reconstructed on a 256 × 256-pixel matrix. Seeds were placed inside high-density upholstery foam, and all experiments were performed at 25 °C. To improve visualization quality, the images were subsequently treated in Matlab, with a scale of 64 colours, to show water distribution with two-dimensional interpolation. The chosen spin-echo sequence for acquiring NMRIs has excellent contrast for free water, i.e., image brightness is proportional to water content. However, monochromatic distribution maps, such as those in shades of grey, are challenging to visualize. Therefore, we utilized a pseudo-colour map in Matlab (Jet colormap) and applied a 5% threshold, representing only regions above this threshold in colour.

Scanning electron microscopy (SEM)

For visualization of seed tissues/parts and composites of XyG/cellulose, cellulose, and XyG alone, samples were mounted on stubs, freeze-dried, and coated with gold (Baltec SCD 050 coater). SEM was also used to visualize different tissues within the seed. Because it is well known that storage XyG is in cotyledonary cell walls, we indirectly identified its presence in these cell walls. Materials were photographed in an SEM XL20 (Philips).

Extraction of water-soluble carbohydrates

Seed coats and cotyledons from three quiescent seeds were mechanically separated, dried in an oven at 60 °C for 24 h, and powdered in a ball mill (n = 3). The powdered cotyledons and seed coats (100 mg) were extracted in 30 ml water at 80 °C for 8 h. After filtration through nylon cloth, the solution was centrifuged (10,000 ***g***, 30 min, 5 °C), precipitated with three volumes of ethanol, and incubated overnight at 5 °C. The precipitate was collected by centrifugation, freeze-dried, and weighed. The water-soluble polysaccharides obtained from cotyledons produce a 'fluffy' material that is >90% XyG (Buckeridge *et al.* 1992). The monosaccharide composition was assessed by acid hydrolysis with 72% (w/w) H_2SO_4 at 30 °C for 45 min, followed by 4% (w/w) H_2SO_4 for 1 h at 120 °C (Saeman *et al.* 1945). After acid hydrolysis, the samples were neutralized with NaOH (50%) and desalted in an anionic (Dowex 1× 8–200) and cationic (Dowex 50× 8–200) ion-exchange column.

Lignin quantification in the seed coat

The seed coat (30 mg) was treated with 1 mL water, 100% ethanol, ethanol-chloroform (1:1 v/v), and 100% acetone (Van Acker *et al.* 2013) to remove soluble sugars and impurities. The samples were incubated for 15 min with stirring of 750 rpm at 98, 76, 59, and 54 °C, respectively, for each reagent. The precipitated material was recovered by centrifugation for 5 min at 14,000 *g* and dried at 45 °C for 2 h.

The lignin content was determined using the acetyl bromide method (Fukushima & Kerley 2011), in which 25% acetyl bromide in acetic acid was added at the 5 mg cell wall sample and incubated for 2 h at 50 °C and 1 h with stirring. Samples were cooled in an ice bath and centrifuged (15 min at 10,000 *g*). The lignin quantification was performed with 2 M sodium hydroxide, 0.5 M hydroxylamine hydrochloride, 100% glacial acetic acid, and acetyl-bromide supernatant solution. Absorbance was read at 280 nm, and lignin content was calculated as a proportion of cell wall biomass, as described by Xue *et al.* (2008).

Fractionation of seed coat cell walls

Soluble sugars were extracted from the powdered seed coats (8 replicates of 400 mg each) in 80% (v/v) ethanol in water at 80 °C for 20 min (Dubois *et al.* 1956), then starch was extracted with rapid stirring in 90% DMSO (Carpita & Kanabus 1987). After these extractions, the cell wall samples were fractionated as described in Gorshkova *et al.* (1996) with modifications. Pectin extraction was performed three times for 1 h in 25 ml aqueous 0.5% ammonium oxalate (pH 7.0) at 80 °C. Insoluble material was pelleted by centrifugation at 13,000 *g* for 15 min. The supernatants were combined and dialyzed for at least 48 h against deionized water, then freeze-dried. Samples were washed with distilled water, and aromatic residues were oxidized by extraction in 0.34 M sodium chlorite in 65 mM acetic acid for 2 h at 80 °C (Carpita 1984). Supernatants were separated, dialyzed, and freeze-dried. Sequentially, the precipitated materials were extracted three times in 25 ml 0.1, 1.0, and 4.0 M NaOH, each supplemented with 3 $mg \cdot ml^{-1}$ $NaBH_4$. The suspensions were stirred at room temperature for 1 h. The supernatants of the NaOH extractions were chilled, acidified with glacial acetic acid, and dialyzed for 48 h against deionized water. Samples were freeze-dried and weighed. Each fraction was assayed colorimetrically for uronic acids (Filisetti-Cozzi & Carpita 1991).

Non-cellulosic monosaccharide composition of cell walls

The non-cellulosic monosaccharide composition of seed coat extracts was determined in 1 mg samples by hydrolysis in 2 M trifluoracetic acid (TFA) for 1 h at 120 °C. After hydrolysis, samples were dried under vacuum (Speedvac; Thermo Scientific Savant SC 250 EXP), resuspended in 1 ml ultrapure water, and filtered through 0.22 µm (Merck Millipore) filters. The monosaccharides were analysed by high-performance anion-exchange chromatography (HPAEC) on a CarboPac SA-10 column (Dionex-Thermo, ICS 5,000 system) by isocratic elution with 99.2% of water and 0.8% 150 mM NaOH ($0.5\ ml \cdot min^{-1}$), followed by 500 µM NaOH post-column ($0.5\ ml \cdot min^{-1}$). Sugars were detected using a pulsed amperometric detector (PAD Dionex-Thermo). Detector responses were determined with the appropriate standards to calculate concentration-response factors for arabinose, xylose, galactose, fucose, mannose, rhamnose, and glucose (De Souza *et al.* 2013).

Linkage analysis of seed coat cell walls

Methylation analysis was carried out on polysaccharide material from oxalate, chlorite, 0.1, 1.0, and 4.0 M NaOH fractions of the seed coat. The samples (10 mg) were delignified with

1 ml 340 mM $NaClO_2$ in acetic acid pH 5.0 for 1 h at 65 °C. Uronosyl residues of pectic polysaccharides in the ammonium oxalate extracts were activated with a water-soluble diimide in 100 mM Na acetate, pH 4.5, and reduced with $NaBD_4$, as described previously (Kim & Carpita 1992), and modified by Carpita & McCann (1997). All materials were dialyzed against distilled water, freeze-dried, and stored over P_2O_5 in a vacuum desiccator for at least 24 h.

For monosaccharide analysis after carboxyl reduction, 1 mg samples of freeze-dried material were hydrolyzed in 2 M TFA at 120 °C for 90 min. Monosaccharides were reduced with $NaBH_4$, and alditol acetates were prepared as described previously (Gibeaut & Carpita 1991), as modified by Mertz *et al.* (2012). Gas–liquid chromatography (GLC) separated derivatives on a 0.25 mm × 30 m column of SP-2330 (Supelco, Bellefonte, PA, USA). Temperature was held at 80 °C for 1 min following injection, then ramped quickly to 200 °C at 25 °C·min^{-1}, then to 240 °C at 5 °C min^{-1} with a 10-min hold at the upper temperature. Helium flow was 1 ml·min^{-1} with splitless injection. Electron impact mass spectrometry (EIMS) was performed with an Agilent MSD at 70 eV and a source temperature of 250°C. The proportions of 6,6-dideuterio-glucosyl and -galactosyl were calculated using pairs of diagnostic fragments *m/z* 187/189, 217/219, and 289/291 according to the equation described in Kim & Carpita (1992) that accounted for spillover of ^{13}C.

For linkage analysis, samples were methylated with *n*-butyllithium and methyl iodide, as described in Gibeaut & Carpita (1991). Partly methylated alditol acetates were separated by GLC on a 30 × 0.25 m capillary column SP-2330 (Supelco). Splitless injections in a helium carrier gas of 1 ml min^{-1} were at 80 °C with a 1-min hold, then ramped to 170 °C at 25 °C·min^{-1}, and then to 210 °C at 2 °C·min^{-1}, then to 240 °C at 5 °C·min^{-1} with a 10-min hold at the upper temperature. Electron-impact mass spectrometry was performed at 70 eV and a source temperature of 250 °C, as in Carpita & Shea (1989). Uronosyl residues were differentiated from their respective neutral sugar by increases of 2 amu in *m/z* values diagnostic of linkage after correction for ^{13}C spillover (Carpita & McCann 1997).

In vitro imbibition of water by polysaccharide composites

To evaluate the effect of water-soluble storage XyG on seed imbibition, composites of 20: 80% (w/w) and 40: 60% (w/w) XyG: cellulose compared to cellulose and XyG matrices alone were used. Imbibition rates were also determined with 30:70% (w/w) *Hymenaea* seed coat chelator-soluble material: cellulose. The cellulose used in this work was obtained by washing milled Whatman number 1 filter paper. The chelator-soluble material used in the composite was from the ammonium oxalate fraction of the seed coat, which was dialyzed against distilled water (15 changes over 5 days) and freeze-dried. Dry samples of each polysaccharide were weighed separately and mixed with cellulose to fill half the height of a 1-mL pipette tip (250 mg of composite or pure polymer). Next, each mixture was suspended in 500 µl distilled water, freeze-dried, and mounted in pre-weighed 1 ml pipette tips (5 tips per sample). This procedure was designed to avoid damage or loss of parts of the composites because of manipulation and to simulate a single water-entrance point, i.e., analogous to experiments with seeds of *Hymenaea*. The tips were kept at 25 °C on a tip-holding tray partially filled with distilled water containing 0.025% sodium azide to prevent microbial degradation. Periodically, the tips were surface dried by paper blotting, weighed, and returned to the same imbibition conditions until constant fresh mass was obtained.

RESULTS

Seed imbibition

Seeds of *Hymenaea* were partially scarified to allow water uptake, whereas non-scarified seeds did not imbibe water (not shown). Imbibition followed a sigmoidal function, reaching maximum imbibition after a minimum of 150 h (6 days), doubling fresh mass (Fig. 1A, Figure S2). However, when the seed coat, embryonic axis, and cotyledons were examined separately, the coat and embryonic axis imbibed water much more quickly, reaching maximum water content in about 5 h (Fig. 1B). In contrast, cotyledons imbibed water more slowly than seed coat and axis, reaching a plateau at about 25 h. The cotyledons represent ca. 70% of dry mass (3.4 ± 0.3 g) in *Hymenaea* seeds compared to 29% (1.4 ± 0.3 g) for the coat and <1% (0.02 ± 0.01 g) for the embryonic axis (Fig. 1C). Thus, water uptake by cotyledons determines the pace of imbibition of the whole seed. Even so, maximum imbibition of seed parts was reached in a fraction of the time necessary for maximum imbibition of the entire seed.

When imbibition is confined to a scarified area of the seed coat, the coat first swelled gradually. However, by time of maximum imbibition, when cotyledons are fully imbibed, the size/volume of the seed had increased considerably, with cracks appearing throughout the coat surface (Figure S2). *Hymenaea* seeds rapidly imbibed fluorescein solution from the scarification point throughout the seed coat, followed by much slower uptake by cotyledons, as observed with brightfield and fluorescence microscopy (Fig. 2). These observations were confirmed and extended with NMRI, showing that water also spread more rapidly through the coat and further to inner cotyledon tissues (Fig. 3). In addition, longitudinal and transverse tomographic section images of the seed showed that water could reach inner portions of the cotyledon before complete imbibition had been achieved (Figure S3).

Seed morphology

The seed coat comprises an outer palisade layer, elongated macrosclereids, an underlying layer of osteosclereids (also called hourglass cells), and a third layer of parenchyma cells, corresponding to ca. 70% of the entire thickness of the seed coat (Fig. 4A–C). The parenchyma layer comprised large, non-isodiametric cells with thin walls (Fig. 4C). Cotyledons contained radially aligned parenchyma cells (Fig. 4A, D). These cells were less densely packed than the parenchyma cells of the seed coat. The cotyledon cells were interlinked by large pit fields (Fig. 4D). At higher magnification, striations in the primary cell wall and channels formed by the intercellular spaces were observed (Fig. 4D, E).

Cell wall composition of the seed parts

Hot water-soluble polysaccharides of cotyledons represented 54% of the dry mass. In contrast, they comprised only 13% of

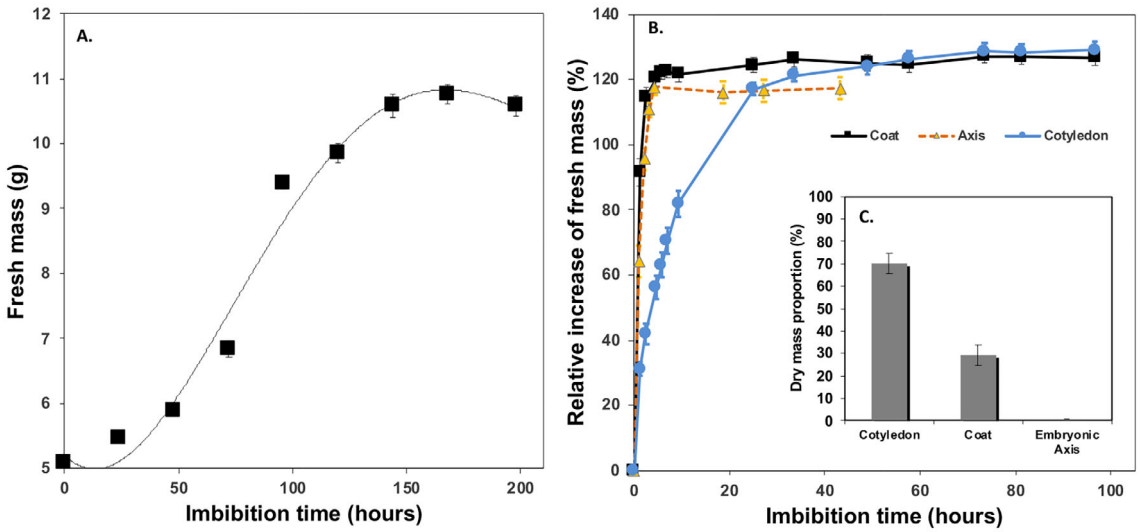

Fig. 1. Rates of imbibition of scarified seeds and isolated *Hymenaea* seed organs. (A) Increment of fresh seed mass (g) Values are mean ± SD (n = 10). (B) The relative increase in fresh mass (weight %) of isolated cotyledons (blue), seed coats (black), and embryonic axes (orange) during imbibition at 20 °C. Values are mean ± SD (n = 15). (C) Proportion of dry mass of isolated cotyledons, seed coat, and embryonic axis. Values are mean ± SD (n = 30).

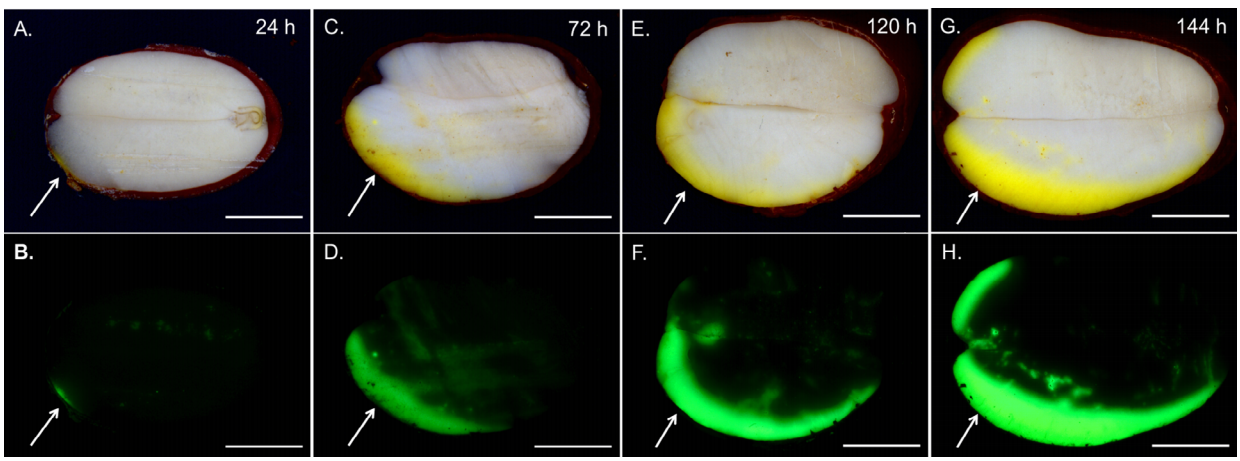

Fig. 2. Longitudinal sections of scarified seeds of *Hymenaea* at different times of imbibition. Arrows represent scarification point and the single water entrance with fluorescein during the experiment. A, C, E, and G are images of seeds at increasing times. Yellow colour is water entrance in cotyledons. B, D, F, and H are fluorescence images at these time points using the stereomicroscope with the GFP filter at 470 nm. Bars represent 5 mm.

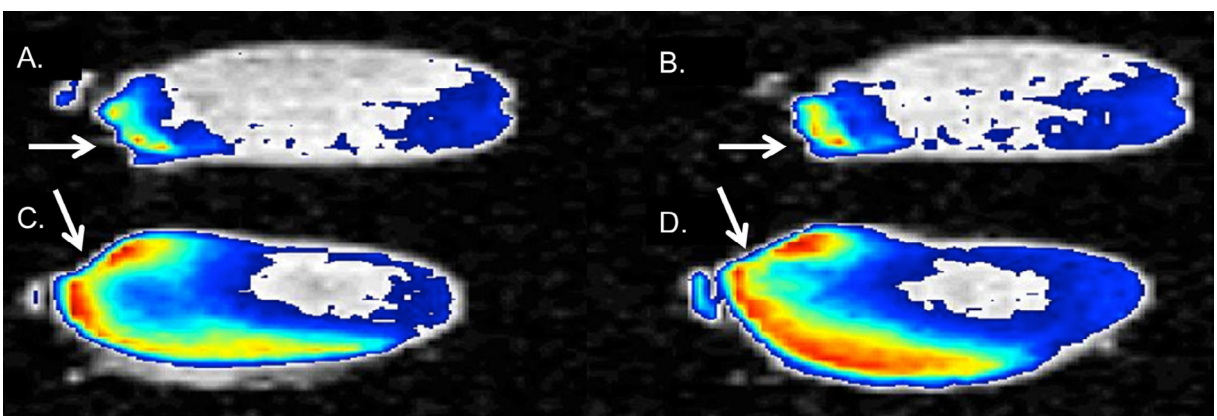

Fig. 3. Magnetic resonance image shows changes in distribution of water in *Hymenaea* seeds over 4 days. (A) 48 h of imbibition, (B) 72 h of imbibition, (C) 96 h of imbibition, (D) 120 h of imbibition. Increases in relative water content are represented by the change from blue to red; white colour refers to <5% of water. Arrows represent the scarified point.

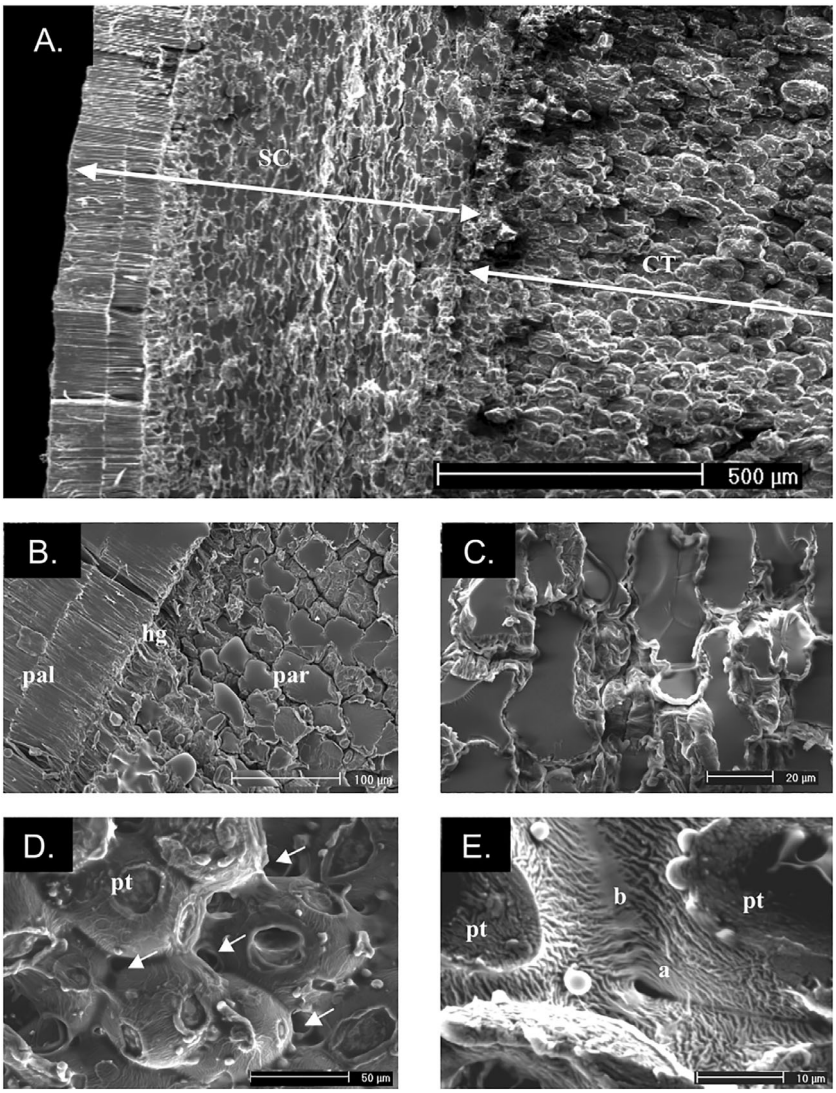

Fig. 4. Scanning electron micrographs showing details of a cross-section of a *Hymenaea* seed. (A) lower magnification showing the seed coat (SC) and part of the cotyledon (CT). Scale bar = 500 µm. (B) Seed coat palisade (pal) layer, osteosclereids cell layer (hg), and parenchyma layer (par). Scale bar = 100 µm. (C) Detail of parenchyma layer of seed coat. Scale bar = 20 µm. (D) Detail of cotyledon cells, showing one out of many pit fields through which cells are linked together (pt). Arrows show the many intercellular spaces. Scale bar = 50 µm. (E) Higher magnification of cotyledon storage cell walls showing the intercellular space (a), deposition of pectin onto microfibrils in a pit field zone between linked cells (b), and detail of a pit field (pt). Scale bar = 10 µm.

the dry mass of the seed coat (Table 1), with the remainder of the dry mass in cell wall polysaccharides and lignin. Lignin was found only in the seed coat and comprised 21.7% of the cell wall mass (Table 1). Uronic acids represented 43% of water-soluble polysaccharides of the seed coat. compared to only 2% in cotyledons. Neutral monosaccharides Glc and Xyl accounted for 88% and 62%, respectively, of the hot water-soluble polymers from cotyledons and seed coats (Table 1). Arabinose (Ara) represented 28 mole % of seed coat monosaccharides but was not detected in the cotyledons.

The cell wall remaining after hot water extract was fractionated sequentially in hot ammonium oxalate (AmmOx) to yield chelator-soluble pectins, then acidic sodium chlorite to oxidize phenylpropanoids and lignins, and increasing concentrations of NaOH to extract additional esterified pectin and hemicelluloses. The AmmOx and chlorite treatments extracted about 20% of total wall mass. In contrast, each alkali fraction yielded about 10% of wall mass, leaving a cell wall residue accounting for 30% of the starting material (Table 2). The chelator-soluble AmmOx fraction yielded mostly uronic acids, Ara, and Xyl. The subsequent chlorite fraction yielded about the same amounts of uronic acid and Xyl but was significantly enriched in Ara compared to the AmmOx fraction (Table 2). Ever-decreasing amounts of uronic acid and arabinose were found in fractions of increasing alkalinity.

In contrast, large amounts of Xyl were detected in all fractions, representing 90% of the total extractable Xyl of the seed coat (Table 2). The residue comprised lignin and cellulose, but 2 M TFA hydrolyzed small amounts of Ara, Gal, uronic acid, and other monosaccharides. Glucose represented a small proportion of all fractions except the 4 M NaOH fraction (Table 2).

Table 1. Composition of water-soluble polysaccharides and lignin from cotyledons and seed coat of *Hymenaea*.

	Water extraction	
	Cotyledons	Coat
Yield ext. (%)[a]	54 ± 8.1	13 ± 0.4
Uronic Ac. (%)[b]	2 ± 1.3	43 ± 0.9
Lignin (%)[c]	–	22 ± 1.1
Monosaccharides (%)	Cotyledons	Coat
GLC	53	27
GAL	11	10
XYL[d]	35	35
FUC	<0.5	<0.5
ARA	n.d.	28
RHA	n.d.	n.d.

Monosaccharide values are the mean ± SD of 3 samples; the lignin value is the mean ± SD of 5 samples.
[a]Values are weight % of dry mass.
[b]Values are weight % of total yield.
[c]Values are weight % of total cell wall.
[d]Xylose values include trace contamination with mannose according to analysis by GC-MS.

Monosaccharide and linkage analyses of each fraction, after carboxyl reduction with $NaBD_4$ to include uronic acids, were consistent with the HPAEC analysis (Tables S1 and S2). Over half of the AmmOx fraction was 4-GalA and its branched residues, indicating homogalacturonan (HG) and xyloHG comprised most of the material. Linkage analysis showed that 2- and 2,4-Rha*p* and 5-Ara*f*, typically associated with the pectic rhamnogalacturonan-I (RG-I), and 4-Xyl*p* and its branched residues, and *t*-Ara*f* and *t*-GlcA, attributed to glucuronoarabinoxylan (GAX) were also detected in lesser amounts (Table S2). In chlorite and increasing alkali extractions, the characteristic RG-I-associated 5-arabinan and GAX residues became more prevalent as decreasing amounts of 4-GalA*p* associated with HG were observed (Table S2). Only in the 4 M alkali extracts were substantial linkage groups associated with XyG, 4- and 4,6-Glc, 2-Xyl, and *t*-Fuc observed.

From linkage analysis (Table 2), the abundance of the major polysaccharides as mole % of polymer diagnostic linkages (Table S3) and their contributions to each fraction and the total could be determined (Fig. 5; Table S4). Over 75% of the seed coat polysaccharide comprised 5-arabinan, GAX, and HG, with smaller amounts of RG-I and XyG (Fig. 5A). Much of the HG is found in the hot water-soluble fraction (Table 1). However, the remainder in the cell wall was mainly extracted by AmmOx or chlorite (Fig. 5B). RG-I and arabinan were abundant in all extracts but were enriched in the 0.1 and 1.0 M NaOH fractions. GAX was also abundant in all fractions but enriched in the alkali fractions, peaking at >60% of material in the 1 M NaOH fraction. The fucosylated XyG was exclusively enriched in the 4 M NaOH fraction (Fig. 5B).

Degrees of branching of RG-I extracted by AmmOx, chlorite, and 0.1 M NaOH indicate that about one-third of the Rha*p* residues bear a side-group, with 5-arabinan as the most likely polymer substituents. Some variation in the degree of branching of 5-arabinan is also evident, with unbranched arabinan representing about two-thirds of the polymer and arabinans with slightly higher branching extracted in the chlorite and 0.1 M NaOH fractions. However, over 80% of the arabinan in the 1.0 M fraction was unbranched. The degree of branching in GAX was about one-third of the polymers extracted by AmmOx and 4 M NaOH, with slightly higher degrees of substitution indicated in chlorite, 0.1, and 1.0 M NaOH fractions (Table S3).

Water imbibition by cellulose/polysaccharide composites

We evaluated water uptake rates and total waterholding capacity using artificial composites with cellulose (Whatman no.1 filter paper) made with the AmmOx pectins or cotyledon unfucosylated storage XyG. Composites were made with pectin:cellulose of 30:70% (w/w) and two different proportions of XyG:cellulose of 20:80% (w/w) and 40:60% (w/w). They were used to compare their pattern of water imbibition with those from cellulose and XyG matrices alone. SEM showing bundles of cellulose microfibrils were well defined in control, but XyG polymers formed homogenous matrices (Fig. 6A, B). When XyG solutions were added to suspensions of cellulose to 20% and 40% (v/w), the microfibril bundles became matted with

Table 2. Cell wall monosaccharide composition of the seed coat of *Hymenaea*.

	Neutral and acid monosaccharides, and yield of cell wall fractions ($mg \cdot g^{-1}$)					
	AmmOx	Chlorite	0.1 M NaOH	1 M NaOH	4 M NaOH	Residue
Fucose	0.6 ± 0.1	2.4 ± 0.2	1.2 ± 0.2	0.7 ± 0.1	6.0 ± 0.4	1.1 ± 0.1
Arabinose	41.0 ± 6.2	337.9 ± 22.8	228.1 ± 12.5	161.0 ± 6.4	143.7 ± 10.8	90.1 ± 6.0
Galactose	3.2 ± 0.5	33.0 ± 3.4	18.9 ± 1.4	7.1 ± 0.7	28.9 ± 1.7	11.3 ± 0.7
Rhamnose	1.6 ± 0.3	8.8 ± 0.8	5.0 ± 1.4	0.9 ± 0.3	3.1 ± 0.3	2.8 ± 0.2
Glucose	0.9 ± 0.1	7.2 ± 0.7	2.2 ± 0.1	3.4 ± 0.5	22.7 ± 1.4	8.6 ± 0.5
Xylose	37.2 ± 7.1	44.8 ± 4.6	224.9 ± 13.9	372.9 ± 15.9	226.9 ± 16.8	6.0 ± 0.4
Mannose	n.d.	1.7 ± 0.1	0.4 ± 0.1	0.12 ± 0.1	0.7 ± 0.2	n.d.
Uronic acids	125.2 ± 15.2	127.5 ± 16.7	114.7 ± 10.1	83.9 ± 8.7	74.6 ± 14.7	32.2 ± 5.9
Yield (% CW)	20.5 ± 0.8	20.7 ± 0.9	10.6 ± 0.4	10.2 ± 0.4	9.1 ± 0.8	29.5 ± 1.2

Cell wall yield (% CW) as the percentage of polysaccharides obtained after dialysis from total dry mass. Uronic Acids ($mg \cdot g^{-1}$) were determined as described (Filisetti-Cozzi and Carpita, 1991). Values are the means ± SE (n = 8) based on standard curves for each HPAEC-PAD monosaccharide. Sugar yields are $mg \cdot g^{-1}$ for all hydrolyzed material in each cell wall fraction. AmmOx = chelator-soluble polysaccharides; Chlorite = polysaccharides extracted by acidic sodium chlorite, and 0.1, 1, and 4 M NaOH = materials extracted by increasing alkali concentrations. Residue = material remaining unextracted by 4 M NaOH. n.d. = not detected.

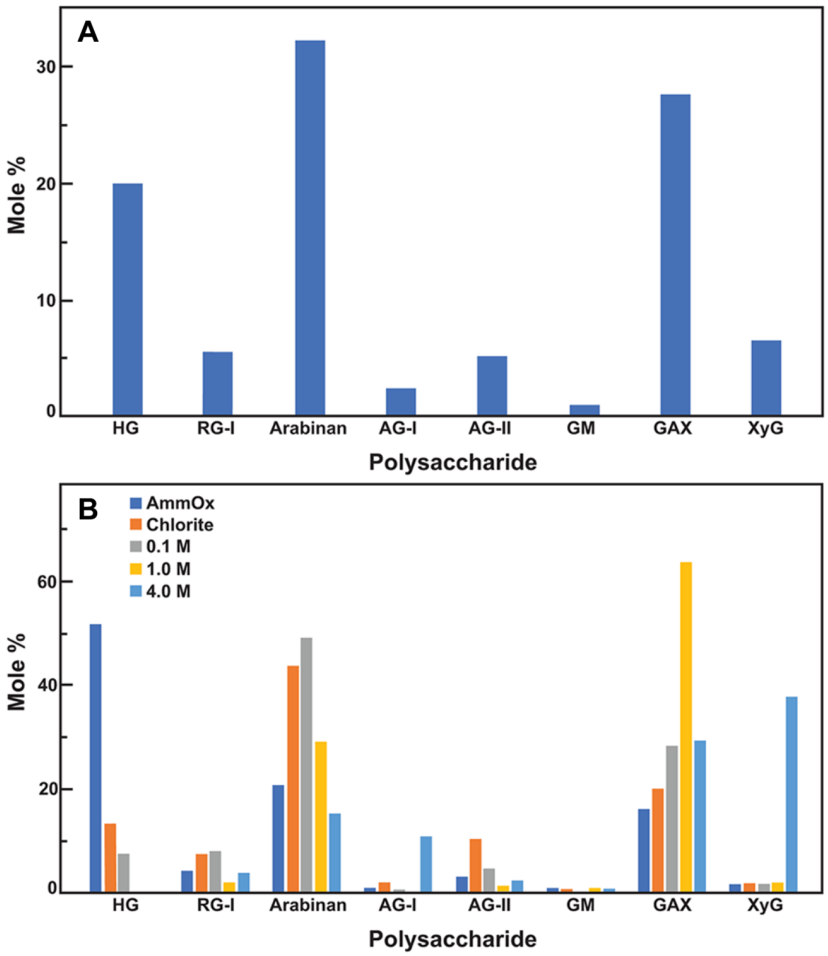

Fig. 5. Polysaccharides of the seed coat of *Hymenaea*. (A) Mole % of Homogalacturonan (HG), rhamnogalacturonan-I backbone (RG-I), 5-arabinan, type I arabinogalactan (AG-I), type II arabinogalactan(-protein) (AG-II), glucomannan (GM), glucuronoarabinoxylan (GAX), and xyloglucan (XyG). Assignments of linkage structures to these polysaccharides (Table S2) are described in Table S3, with proportions of each relative to contributions of dry weight to each fraction in Table 2. (B) Relative proportions of each polysaccharide in various fractions after sequential extraction in hot ammonium oxalate (AmmOx), acidic sodium chlorite (Chlorite), 0.1, 1.0, and 4.0 M NaOH.

matrix polysaccharides, with composites with 40% (v/w) XyG, resembling matrices formed by XyG alone (compare Fig. 6C, D).

To determine the rate of water uptake and the maximum amount of water imbibed, we packed 1 ml disposable pipette tips with XyG and cellulose alone or as their composites and placed them in tubes with 0.5 ml water. We then weighed them periodically until near-maximum absorption had occurred. In cellulose controls, water was taken up within 1 h (Fig. 6E). Water uptake was even more rapid in composites of cellulose and the chelator-soluble pectins and GAX, but maximum absorption did not exceed 40% (v/w). In contrast, water uptake by XyG alone was extremely slow, reaching <20% (v/w) after 30 h (Fig. 6E). Composites of cellulose and XyG showed slower water uptake rates than cellulose alone. However, the addition of 20% (w/w) and 40% (w/w) XyG with cellulose significantly increased the waterholding capacity of the composites compared to cellulose alone or cellulose:pectin composites, with 20% cellulose:80% pectin (w/w) increasing the waterholding capacity to almost 80% (v/w).

DISCUSSION

How do *Hymenaea* seeds imbibe water?

Under optimal conditions, the uptake of water by most seeds exhibits triphasic behaviour. Phase I is the most rapid and is a consequence of the matric forces of hydrophilic cell walls. Once the matric potential is saturated, a subsequent slower period, called Phase II, ensues, in which cellular and membrane integrity is established to become osmotically competent (Bewley & Black 1994; Buckeridge *et al.* 2004; Manz *et al.* 2005). In Phase III, the developed osmotic forces drove the early growth and emergence of the radicle. In legume seeds with permeable seed coats, such as peas (Waggoner & Parlange 1976) and soybean (Leopold 1980; Vertucci & Leopold 1983; McDonald Jr *et al.* 1988a, 1988b), Phase I of water uptake is so rapid that the imbibition curve displays a hyperbolic shape with a much longer Phase II. However, for hard-coated seeds with water-impermeable coats, such as *Hymenaea*, water entry begins only when the coat surface can be breached upon degradation by microorganisms. To study

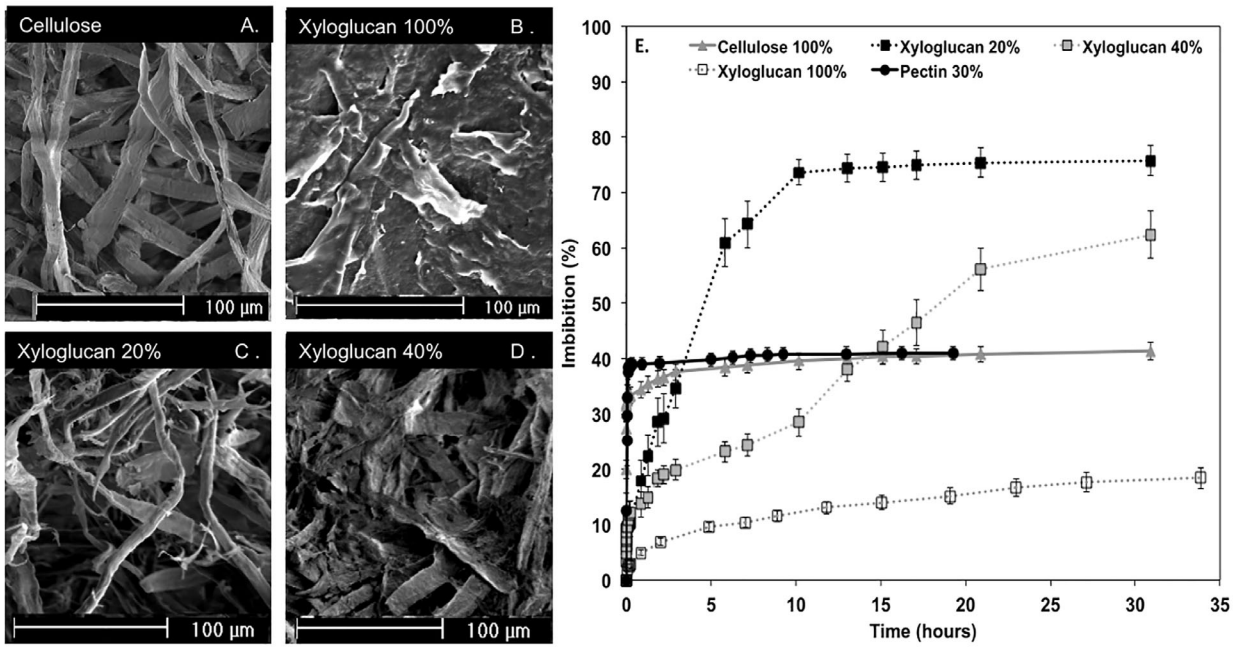

Fig. 6. Scanning electron micrographs show differences between matrices and composites of cellulose and xyloglucan. (A) 100% cellulose; (B) 100% xyloglucan; (C) 20% of xyloglucan in cellulose; (D) 40% of xyloglucan in cellulose. Scale bar = 100 µm. (E) Time course of imbibition of cellulose, 100% xyloglucan, and composites of pectin:cellulose (30:70%) and xyloglucan:cellulose (20:80% and 40:60%). The pectin and xyloglucan were extracted from seed coats and cotyledons, respectively, of *Hymenaea* seeds. Data are mean ± SD of 5 samples.

water movement in these seeds, the seed coat is scarified, or mechanically broken, usually near the embryonic axis (Souza & Válio 2001). Even after scarification, Phases I and II are fused into a monophasic sigmoidal curve, mainly due to the cotyledons' slow water absorption. In *Hymenaea*, different seed parts imbibe water at different rates. Whereas the seed coat and the axis imbibe water quickly, the cotyledons absorb water more slowly. Here, we show that the differing rates of water absorption result from the polysaccharide constituents of the cell walls of all seed tissues.

We found that imbibition is a two-step process in *Hymenaea*, the first dominated by rapid hydration of the entire seed coat and the second by slower, more uniform hydration of the cotyledons. Typical of seeds of the Caesalpinioideae (Flores 1990), the seed coat of *Hymenaea* is a multi-layered structure, including both macro- and osteosclerids in its outer integument and parenchyma in its inner integument (van Dongen *et al.* 2003; Verdier *et al.* 2012). The palisade layer is often regarded as a barrier to water entry into the hard-coated seed, mainly due to lignified cell walls (Esau 1977; Flores 1990). The layer of osteosclereids, which is usually found in relatively high proportions in the seed coat of legume species of Papilionoideae, such as common bean (*Phaseolus vulgaris* L.) (Esau 1977) and soybean (*Glycine max* L.) (McDonald Jr *et al.* 1988a,b), is thought to be a vector of radial water distribution throughout the seed coat. The relatively reduced proportion of osteosclereids cells in *Hymenaea* (~4% of the seed coat) is balanced by an increase in the thickness of the underlying parenchyma layer. In six soybean cultivars, the cuticle of the palisade layer determines water permeability (Ma *et al.* 2004). The cuticle of an impermeable seed coat is mechanically robust and does not crack under normal circumstances. However, when this palisade is mechanically weak, the coat develops small cracks through which water can pass (Ma *et al.* 2004). Following imbibition, the parenchyma layer expands to twice its thickness. As a consequence of cell expansion, the palisade layer ruptures, introducing new openings in the seed coat and allowing enhanced water uptake. Underlying the primary wall, the very thick storage cell walls of the cotyledon, rich in XyG (Tiné *et al.* 2000a), absorb water much more slowly but display a series of intercellular connections that direct passage of water from cell to cell via storage walls (Tiné *et al.* 2000b).

Cell wall composition of the seed coat

The seed coat walls are enriched in HG, RG-I decorated with arabinan, and GAX, polymers whose hydrophilic properties are responsible for the rapid hydration and swelling. The RG-I functions as a scaffold for the pectins (Vincken *et al.* 2003; Ulvskov *et al.* 2005), upon which a diverse array of monosaccharide and oligomeric substitutions are found in cell- and developmental stage-specific patterns. The swelling potentials of HG and RG-I are well established. RG-I, a significant component of seed mucilage, swells to form gels spontaneously upon soaking in water (Haughn & Western 2012). Seed mucilages from white mustard (*Brassica alba*) and cress (*Lepidium sativum*) are also rich in RG-I branched with Ara and Gal (Bailey & Norris 1932; Bailey 1935). Seed mucilage of plantain (*Plantago psyllium*) has a neutral arabinoxylan and RG-I (Jones & Albers 1955). Arabidopsis (*Arabidopsis thaliana*) seed mucilage is composed almost exclusively of RG-I, with a low frequency of side branching with both 5-arabinans and non-reducing terminal galactosyl residues (Macquet *et al.* 2007). Flax (*Linum usitatissimum*) seed mucilage is enriched with RG-

I but, like plantain, also contains the neutral arabinoxylan (Naran *et al.* 2008). The neutral arabinoxylan is also distinctive for a lack of *t*-GlcA residues and a higher degree of 'double-arabinosylation,' where two L-Ara units are attached to the *O*-2 and *O*-3 positions of the 4-Xyl residues. The lower pectin content of soybean reduces the seed coat's hydrophilic properties (Mullin & Xu 2001).

The seed coat of *Hymenaea* also contains RG-I but, like flax, has an acidic arabinoxylan. However, the *Hymenaea* RG-I displays an unusually high degree of substitution with 5-arabinan side chains that might also contribute to the swelling and water-transport properties of the composite confined in a primary cell wall of the seed coat. For example, the 5-arabinans are typically enriched in meristematic cells, whereas 4-galactans appear during elongation as 5-arabinans disappear (Bush *et al.* 2001).

Arabinans impart the wall flexibility required for the reversible opening and closing of guard cells (Jones *et al.* 2003). A unique role for 5-arabinans in maintaining wall flexibility during desiccation tolerance has also been proposed (Moore *et al.* 2008). Lines of transgenic potato (*Solanum tuberosum*) with reduced arabinan content lost water more rapidly from tuber discs exposed to strain, implicating arabinan in water retention as well as solubility (Ulvskov *et al.* 2005). Relevant to *Hymenaea*, water-retention properties of arabinans in cell walls contribute to the hydration of the seed endosperm of honey locust (*Gleditsia triacanthos*) during germination (Navarro *et al.* 2002). Solid-state NMR studies show that the arabinan side chains hydrate more readily than galactan side chains, indicating that the overall hydration properties of pectin gels can be controlled by modifying the ratio of these side chains enzymatically (Larsen *et al.* 2011). Thus, the RG-Is of the *Hymenaea* seed coat share the same hydration and gelling properties as seed mucilages but are confined by the seed coat. The forces generated by gelation are sufficient to introduce cracks in the seed coat that provide new routes for water entry.

Hydration of the cotyledons is the rate-limiting phase of imbibition

While the seed coats absorb and distribute water quickly around the periphery of the cotyledons, the absorption of water by the cotyledons is much slower. Pectin composites extracted in the chelator-soluble fraction of the coat or pure cellulose absorb water faster than *Hymenaea* XyG from the cotyledon cell walls. *Hymenaea* XyG alone absorbs <20% (v/w) of the available water *in vitro*, but composites made by coating cellulose microfibrils with only 20% (w/w) XyG enhance total water uptake to almost 80% (v/w), almost twice that of cellulose alone or cellulose-pectin composites. As imaged by SEM, the cellulose fibrers became barely distinguishable when XyG is added to the cellulose fibrers at a proportion of 40% (w/w). These results are consistent with those that show that XyG binds to cellulose and that their composites form stiff matrices with increased elastic properties compared to cellulose alone (Whitney *et al.* 1995, 1998; Lima & Buckeridge 2001).

Although the chemical properties of the pectin composites result in rapid water uptake and gel formation, those of the XyG-cellulose matrix of the cotyledon cell wall significantly increase waterholding capacity. Despite the fast distribution of water to all surfaces of the cotyledon, the slower uptake of water by the XyG-cellulose matrix requires a network of capillary channels present in intercellular spaces to facilitate water movement throughout the cotyledon, a feature that has been reported in several leguminous seeds, including *Hymenaea* (Reid & Bewley 1979; Buckeridge *et al.* 2000a; Lima *et al.* 2003). *Hymenaea* cotyledons are rich in XyG as a primary polysaccharide storage polymer (Buckeridge 2010). As with all XyG, those of *Hymenaea* have a cellulose-like (1→4)-β-D-glucan backbone to which single (1→6)-α-D-xylopyranoside substituents are attached (Buckeridge *et al.* 2000b). However, the pattern of xylosyl substitution of XyG from *Hymenaea* is remarkably distinct from other seed XyG. Whereas nasturtium (*Tropaeolum majus*), tamarind (*Tamarindus indica*), and copaifera (*Copaifera langsdorffii*) XyG are composed of repetitive units of glucose$_4$:xylose$_3$ (York *et al.* 1990; Buckeridge *et al.* 1992), *Hymenaea* XyG is composed of a mixture of glucose$_4$:xylose$_3$ and glucose$_5$:xylose$_4$ repetitive units (Tiné *et al.* 2006), illustrating how polysaccharide and composite structures are modified to optimize function at many levels, an idea captured in the 'Glycomic Code' (Buckeridge 2018). Also, the hydration properties and enzymatic degradation pathways of XyG depend on the degree and pattern of Gal substitution inherent in these storage XyG. Mutations in primary wall XyG in *Arabidopsis* significantly reduce or eliminate Gal residues, reduce water solubility, and the ability to modify enzymes such as XyG endo-β-transglycosylase to recognize them (Peña *et al.* 2004).

Physiological importance of polysaccharides in the uptake of water by seeds of *Hymenaea*

Based on the results of the rate of imbibition, distribution, and dynamics of imbibition of water in the seed, seed coat polysaccharide composition, hydrodynamic properties of XyG, and ultrastructural observations, we propose a model for water uptake by seeds of *Hymenaea* that might extend to other leguminous species, such as *Tamarindus indica* (Reis *et al.* 1987) and *Copaifera langsdorffii* (Tiné *et al.* 2003). Depending on the species, the thick cotyledon walls of seeds of leguminous plants may accumulate galactomannan or XyG (Buckeridge *et al.* 2000b; Buckeridge 2010) as storage carbohydrates. Both polymers share similar hydrodynamic properties. Galactomannans are directly related to the influence of water uptake by endosperm-containing seeds such as *Trigonella foenum-graecum* (Reid & Bewley 1979), *Dimorphandra mollis*, and *Sesbania virgata* (Buckeridge *et al.* 1995; Buckeridge & Dietrich 1996). Galactosyl substitution and probably acetylation of mannans and galactomannans (Meier & Reid 1982) interfere in controlling the rate and extent of water imbibition by the endosperm. Although seed XyG displays similar physical–chemical features to galactomannan, their role as a water imbibition substance has been less studied.

The seed coat performs two essential functions. First, it quickly absorbs and distributes water to the embryonic axis and over the entire surface of the cotyledons. Second, the swelling of the gel matrix of the palisade layer bursts the seed coat to allow water absorption through multiple entry points. On the one hand, its palisade layer, richer in cellulose and lignin, restricts water entry through the hilum or any other region of the seed coat surface. Interactions of lignin, cellulose, and hemicellulose render the tissue a higher degree of brittleness.

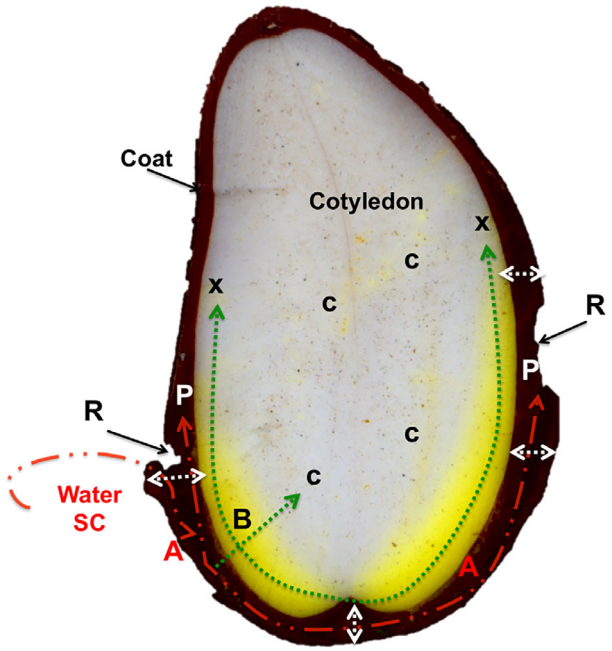

Fig. 7. Model for water uptake mechanisms of *Hymenaea seeds*. After scarification (SC), the water follows primarily route A (red line), which moves faster in the seed coat than in the cotyledons, driven by pectin-rich walls in the parenchyma layer (P). This behaviour promotes expansion of seed coats (double-headed white arrows) and consequently induces ruptures (R) in the palisade layer. These events open new routes for water uptake throughout the seed coat. After the seed coat becomes saturated with water, the waterfront flows more slowly through route B (green lines), moving both through intercellular channels (c) (see Figures S3 and S6) and xyloglucan-containing storage walls (x).

After crossing this barrier, water gains access to the parenchyma layer, which is rich in water-soluble pectin and whose function is to rapidly distribute water around the cotyledon surfaces (Fig. 7). As this pectin-rich layer takes up water, it expands to approximately twice its original volume, promoting ruptures in several regions of the palisade layer and leading to the opening of several new water entry locations. These ruptures are related directly to the progression of the waterfront following route A (Fig. 7). They are faster than the waterfront following route B within the cotyledons. These findings are consistent with our observation that a proportion of the seed coat comprises relatively more water-soluble pectin. In contrast, the primary imbibing substance in cotyledons is XyG, which takes up water slowly. This reflects the distinct differences in water absorption by every seed tissue.

In the cotyledons, route B can be subdivided into two different routes. Route B (c) accounts for the channels formed by intercellular spaces. In contrast, route B (x) is likely associated with water absorption mainly by XyG (Fig. 7). Because of the similarity of the hydrodynamic features of storage galactomannans and XyG (Reid 1985; Buckeridge *et al.* 2000b), the XyG–water interaction produces a highly viscous medium that restricts the advance of water into the matrix. As suggested for galactomannan-containing seeds (Reid & Bewley 1979), the enhanced waterholding capacity of XyG-cellulose matrices might play a role as a water buffer under periods of stress following radicle emergence.

CONCLUSION

The seed cell wall polysaccharides of the seed coat and cotyledons of *Hymenaea* are typical of most legume seeds. Our findings demonstrate that cell wall composition is vital to water imbibition in different seed tissues. The entrance of water in the pectin-rich parenchyma layer induces cracks in the lignified palisade layer and feed-backing water imbibition by the seed coat. The parallel waterfronts in the coat and cotyledon cells at different speeds likely promote synchronized activation of the metabolism of the embryo, which is fast, with a slower activation of the metabolism of storage XyG since the latter will take place later during seedling establishment. Thus, the dynamic interactions between water and wall polysaccharides (pectins and hemicellulose) are central to determining water distribution and preparing seedlings for establishment.

AUTHOR CONTRIBUTIONS

Conceptualization, MSB, HPS, AG; methodology and analysis, AG, HPS, PPT ISS ASCP, NCC, MBS; investigation, AG, HPS, PPT ISS ASCP, NCC, MSB; writing–original draft preparation, MSB, AG, HPS, NCC; writing–review and editing, MSB, AG.

ACKNOWLEDGEMENTS

The authors thank RT Shirasuna for technical assistance with the SEM, Dr. Marco Aurélio Tiné and Eglee Igarashi for helping with HPAEC analyses, Dr. Viviane Costa for cell wall extraction and photos from trees, Dr. Debora Pagliuso for lignin analysis. The authors thank Luiz Alberto Colnago, from EMBRAPA, for allowing use of the iNMR equipment. This study was supported by Fundação de Amparo a Pesquisa do Estado de São Paulo-FAPESP (1998/05124-8). This work was partly financed by the National Institute of Science and Technology of Bioethanol / CNPq and Fapesp (CNPq465319/2014-9) and (Fapesp2014/50884-5) and FAPESP fellowship to AG (FAPESP 2019/13936-0).

DATA AVAILABILITY STATEMENT

The data supporting this study's findings are available from the corresponding author upon reasonable request.

SUPPORTING INFORMATION

Additional supporting information may be found online in the Supporting Information section at the end of the article.

Figure S1. *Hymenaea* tree, fruits, and seeds. (A) Mature individual tree; (B) branches and green fruits; (C) mature fruit; (D) transversal section of green fruit and immature seed (ct = cotyledons, co = seed coat, st = farinaceous starch content inside the fruit; fc = fruit coat); and E) mature seeds. (Bars = 2 cm).

Figure S2. Swelling behaviour of *Hymenaea* seeds during imbibition at 25 °C. The arrows represent the single scarification point through which seeds imbibed fluorescein dissolved in water. Bar = 1 cm.

Figure S3. Magnetic resonance image of *Hymenaea* seeds after 144 h of imbibition. (A) Longitudinal section. (B)

Transversal section. Increases in relative water content are represented by a change from blue to red; white colour refers to <5% water. The arrows represent the scarified area.

Table S1. Monosaccharide analysis (%mole) by alditol acetates of extracts of ammonium oxalate (AmmOx), acidic sodium chlorite (Chlorite), and increasing concentrations of alkali from cell walls of the seed coat of *Hymenaea*. Monosaccharide composition was determined after separation and quantitation of alditol acetate derivatives by GC-EIMS. Values are mean ± SD of 3 samples. Galacturonic acid (GalA) and glucuronic acid (GlcA) were carboxyl-reduced with $NaBD_4$ to generate 6,6-dideutero-isomers of Gal and Glc, resolved from their respective neutral sugar by MS (Carpita & McCann 1997). Uronic acids were not determined in 4 M extracts.

Table S2. Linkage analysis of extracts of ammonium oxalate, acidic sodium chlorite, and increasing concentrations of alkali from cell walls of the seed coats of *Hymenaea*.

Table S3. Diagnostic linkage groups determined by gas–liquid chromatography–electron impact mass spectrometry of partly methylated alditol acetate derivatives of polysaccharides. Uronic acids were carboxyl-reduced with $NaBD_4$ to generate 6,6-dideutero-isomers of Gal and Glc resolved from their respective neutral sugar by MS. Polysaccharide abundances were calculated from the sum of the mole% of these diagnostic linkages presented in Tables S1 and S2.

Table S4. Diagnostic linkage groups determined by gas–liquid chromatography–electron impact mass spectrometry of partly methylated alditol acetate derivatives of polysaccharides in *Hymenaea*. Uronic acids were carboxyl-reduced with $NaBD_4$ to generate 6,6-dideutero-isomers of Gal and Glc resolved from their respective neutral sugar by GC-EIMS. Polysaccharide abundances were calculated from the sum of the mole% of the diagnostic linkages presented in Table S2 as defined in Table S3.

REFERENCES

Aidar M.P.M., Martinez C.A., Costa A.C., Costa P.M.F., Dietrich S.M.C., Buckeridge M.S. (2002) Effect of atmospheric CO_2 enrichment on the establishment of seedlings of jatobá, *Hymenaea courbaril* L. (Leguminosae, Caesalpinioideae). *Biota Neotropica*, **2**, 1–10.

Bailey K. (1935) Cress seed mucilage. *Biochemical Journal*, **29**, 2477–2485.

Bailey K., Norris F.W. (1932) The nature and composition of the mucilage of the seed of white mustard (*Brassica alba*). *Biochemical Journal*, **26**, 1609–1623.

Baskin J.M., Baskin C.C., Li X. (2000) Taxonomy, anatomy, and evolution of physical dormancy. *Plant Species Biology*, **15**, 139–152.

Bewley J.D., Black M. (1994) *Seeds – Physiology of development and germination*, 2nd edition. Plenum Press, New York, USA, pp 147–197.

Bradford K.J. (1990) A water relations analysis of seed germination rates. *Plant Physiology*, **94**, 84–849.

Buckeridge M.S. (2010) Seed cell wall storage polysaccharides: models to understand cell wall biosynthesis and degradation. *Plant Physiology*, **154**, 1017–1023.

Buckeridge M.S. (2018) The evolution of the Glycomic codes of extracellular matrices. *Biosystems*, **164**, 112–120.

Buckeridge M.S., Crombie H.J., Mendes C.J.M., Reid J.S.G., Gidley M.J., Vieira C.C.J. (1997) A new family of oligosaccharides from the xyloglucan of *Hymenaea courbaril* L. (Leguminosae) cotyledons. *Carbohydrate Research*, **303**, 233–237.

Buckeridge M.S., Dietrich S.M.C. (1996) Mobilisation of the raffinose family oligosaccharides and galactomannan in germinating seeds of *Sesbania marginata* Benth. (Leguminosae-Faboideae). *Plant Science*, **117**, 33–43.

Buckeridge M.S., Dietrich S.M.C., Lima D.U. (2000a) Galactomannans as the reserve carbohydrate in legume seeds. In: Gupta A.K., Kaur N. (Eds), *Carbohydrate reserves in plants – Synthesis and regulation*. Elsevier Science, Paris, France, pp 283–317.

Buckeridge M.S., Panegassi V.R., Dietrich S.M.C. (1995) Storage carbohydrate mobilisation in seeds of *Dimorphandra mollis* Benth. (Leguminosae) following germination. *Revista Brasileira de Botânica*, **18**, 171–175.

Buckeridge M.S., Rocha D.C., Reid J.S.G., Dietrich S.M.C. (1992) Xyloglucan structure and post-germinative metabolism in seeds of *Copaifera langsdorffii* from savannah and forest populations. *Physiologia Plantarum*, **86**, 145–151.

Buckeridge M.S., Santos H.P., Tiné M.A.S. (2000b) Mobilisation of storage cell wall polysaccharides in seeds. *Plant Physiology and Biochemistry*, **38**, 141–156.

Buckeridge M.S., Santos H.P., Tiné M.A.S., Aidar M.P.M. (2004) Mobilização de reservas. In: Ferreira A.G., Borghetti F. (Eds), *Germinação: do básico ao aplicado*. Artmed, Porto Alegre, Brazil, pp 163–185.

Bush M.S., Marry M., Huxam I.M., Jarvis M.C., McCann M.C. (2001) Developmental regulation of pectic epitopes during potato tuberization. *Planta*, **213**, 869–880.

Callaghan P.T. (1991) *Principles of nuclear magnetic resonance spectroscopy*. Oxford University Press, Oxford, UK, pp 483.

Carneiro F.S., Lacerda A.E.B., Lemes M.R., Gribel R., Kanashiro M., Wadt L.H.O., Sebbenn A.M. (2011) Effects of selective logging on the mating system and pollen dispersal of *Hymenaea courbaril* L. (Leguminosae) in the Eastern Brazilian Amazon as revealed by microsatellite analysis. *Forest Ecology and Management*, **262**, 1758–1765.

Carpita N.C. (1984) Cell wall development in maize coleoptiles. *Plant Physiology*, **76**, 205–212.

Carpita N.C., Kanabus J. (1987) Extraction of starch by dimethyl sulfoxide and quantitation by enzymatic assay. *Analytical Biochemistry*, **161**, 132–139.

Carpita N.C., McCann M.C. (1997) Some new methods to study plant polyuronic acids and their esters. In: Townsend R., Hotchkiss A. (Eds), *Progress in Glycobiology*. Marcell Dekker, New York, USA, pp 595–611.

Carpita N.C., Shea E.M. (1989) Linkage structure by gas chromatography-mass spectrometry of partially-methylated alditol acetates. In: Biermann C.J., McGinns C.D. (Eds), *Analysis of carbohydrates by GLC and MS*. CRC Press, Boca Raton, FL. USA, pp 157–216.

De Souza A.P., Leite D.C.C., Pattathil S., Hahn M.G., Buckeridge M.S. (2013) Composition and structure of sugarcane cell wall polysaccharides: implications for second-generation bioethanol production. *Bioenergy Research*, **6**, 564–579.

Di Stasi L.C., Oliveira G.P., Carvalhaes M.A., Queiroz-Junior M., Tien O.S., Kakinami S.H., Reis M.S. (2002) Medicinal plants popularly used in the Brazilian Tropical Atlantic Forest. *Fitoterapia*, **73**, 69–91.

Dubois M., Gilles K.A., Hamiltons J.K., Rebels P.A., Smith F. (1956) Colorimetric methods for determination of sugars and related substances. *Annals of Chemistry*, **3**, 350–356.

Egley G.H. (1989) Water-impermeable seed coverings as barriers to germination. In: Taylorson R.B. (Ed), *Recent advances in the development and germination of seeds*. NATO ASI Series (Series A: Life Sciences), vol 187. Springer, Boston, MA. https://doi.org/10.1007/978-1-4613-0617-7_16

Esau K. (1977) *Anatomy of plant seeds*, 2nd edition. John Wiley & Sons, New York, USA.

Filisetti-Cozzi T.M.C.C., Carpita N.C. (1991) Measurement of uronic acids without interference from neutral sugar. *Analytical Biochemistry*, **197**, 157–162.

Flores E.M. (1990) Germinación y morfología de la plántula de *Hymenaea courbaril* L. (Caesalpinaceae). *Revista de Biología Tropical*, **38**, 91–98.

Fukushima R.S., Kerley M.S. (2011) Use of lignin extracted from different plant sources as standards in the spectrophotometric acetyl bromide lignin method. *Journal of Agricultural and Food Chemistry*, **59**, 3505–3509. https://doi.org/10.1021/jf104826n

Gibeaut D.M., Carpita N.C. (1991) Tracing the biosynthesis of the cell wall in intact cells and plants. Selective turnover and alteration of cytoplasmic and cell wall polysaccharides of proso millet cells in liquid culture and *Zea mays* seedlings. *Plant Physiology*, **97**, 551–561.

Gorshkova T.A., Wyatt S.E., Salnikov V.V., Gibeaut D.M., Ibragimov M.R., Lozovaya V.V., Carpita N.C. (1996) Cell-wall polysaccharides of developing flax plants. *Plant Physiology*, **3**, 721–729.

Haughn G.W., Western T.L. (2012) Arabidopsis seed coat mucilage is a specialized cell wall that can be used as a model for genetic analysis of plant cell wall structure and function. *Frontiers in Plant Science*, **3**, 64.

Hayashi T. (1989) Xyloglucan in the primary cell wall. *Annual Review of Plant Physiology and Plant Molecular Biology*, **40**, 139–168.

Jones L., Milne J.L., Ashford D., McQueen-Mason S.J. (2003) Cell wall arabinan is essential for guard cell function. *Proceedings of the National Academy of Sciences of the United States of America*, **100**, 11783–11788.

Jones M.J., Albers C.C. (1955) Further studies on Texas plantago seeds. *Journal of the American Pharmacological Association*, **44**, 100–105.

Kim J.B., Carpita N.C. (1992) Changes in esterification of the uronic acid groups of cell wall polysaccharides during elongation of maize coleoptiles. *Plant Physiology*, **98**, 646–653.

Lacerda A.E.B., Nimmo E.R., Sebbenn A.M. (2013) Modeling the long-term impacts of logging on genetic diversity and demography of *Hymenaea courbaril*. *Forest Science*, **59**, 15–26. https://doi.org/10.5849/forsci.10-118

Larsen F.H., Byg I., Damager I., Diaz J., Engelsen S.B., Ulvskov P. (2011) Residue specific hydration of primary cell wall potato pectin identified by solid-state ^{13}C single-pulse MAS and CP/MAS NMR spectroscopy. *Biomacromolecules*, **12**, 1844–1850.

Lee Y., Langenheim J.H. (1975) *Systematics of the genus Hymenaea L. (Leguminosae, Caesalpinioideae, Detarieae)*. University of California Publications in Botany, Berkeley, CA, USA.

Leopold A.C. (1980) Temperature effects on soybean imbibition and leakage. *Plant Physiology*, **65**, 1096–1098.

Lima D.U., Buckeridge M.S. (2001) Interaction between cellulose and storage xyloglucans: the influence of degree of galactosylation. *Carbohydrate Polymers*, **46**, 157–163.

Lima D.U., Oliveira R.C., Buckeridge M.S. (2003) Seed storage hemicelluloses as wet-end additives in papermaking. *Carbohydrate Polymers*, **52**, 367–373.

Lopes S.D., Schiavini I., Oliveira A.P., Vale V.S. (2012) An ecological comparison of floristic composition in seasonal semideciduous forest in Southeast Brazil: implications for conservation. *International Journal of Forestry Research*, **2012**, 537269. https://doi.org/10.1155/2012/537269

Ma F., Cholewa E., Mohamed T., Peterson C.A., Gijzen M. (2004) Cracks in the palisade cuticle of soybean seed coats correlate with their permeability to water. *Annals of Botany*, **94**, 213–228. https://doi.org/10.1093/aob/mch133

Macquet A., Ralet M.C., Kronenberger J., Marion-Poll A., North H.M. (2007) In situ, chemical and macromolecular study of the composition of *Arabidopsis thaliana* seed coat mucilage. *Plant & Cell Physiology*, **48**, 984–999.

Manz B., Müller K., Kucera B., Volke F., Leubner-Metzger G. (2005) Water uptake and distribution in germinating tobacco seeds investigated *in vivo* by nuclear magnetic resonance imaging. *Plant Physiology*, **138**, 1538–1551.

Martin S.S., Langenheim J.H., Zavarin E. (1972) Sesquiterpenes in leaf pocket resin of *Hymenaea courbaril*. *Phytochemistry*, **11**, 3049–3051.

McDonald M.B., Jr., Vertucci C.W., Roos E.E. (1988a) Seed coat regulation of soybean seed imbibition. *Crop Science*, **28**, 987–992.

McDonald M.B., Jr., Vertucci C.W., Roos E.E. (1988b) Soybean seed imbibition: water absorption by seed parts. *Crop Science*, **28**, 993–997.

Meier H., Reid J.S.G. (1982) Reserve polysaccharide other than starch in higher plants. In: Loewus F.A., Tanner W. (Eds), *Plant carbohydrates*. Springer, New York, USA, pp 418–471.

Mertz R.A., Olek A.T., Carpita N.C. (2012) Alterations in cell-wall glycosyl structure of *Arabidopsis murus* mutants. *Carbohydrate Polymers*, **89**, 331–339.

Moore J.P., Farrant J.M., Driouich A. (2008) A role for pectin-associated arabinans in maintaining the flexibility of the plant cell wall during water deficit stress. *Plant Signaling & Behavior*, **3**, 102–104.

Mullin W.J., Xu W. (2001) Study of soybean seed coat components and their relationship to water absorption. *Journal of Agricultural and Food Chemistry*, **49**, 5331–5335.

Naran R., Chen G., Carpita N.C. (2008) Novel rhamnogalacturonan I and arabinoxylan polysaccharides of flax seed mucilage. *Plant Physiology*, **148**, 132–141.

Navarro D.A., Cerezo A.S., Stortz C.A. (2002) NMR spectroscopy and chemical studies of an arabinan-rich system from the endosperm of the seed of *Gleditsia triacanthos*. *Carbohydrate Research*, **337**, 255–263.

Nonogaki H. (2008) Seed germination and reserve mobilization, *Encyclopedia of life sciences*. John Wiley, Chichester, UK, pp 1–9. https://doi.org/10.1002/9780470015902.a0002047.pub2

Peña M.J., Ryden P., Madson M., Smith A., Reiter W.-D., Carpita N.C. (2004) Galactosylation of xyloglucans is essential for maintenance of cell wall tensile strength during cell growth in plants. *Plant Physiology*, **134**, 443–451.

Reid J.S.G. (1985) Structure and function of legume-seed polysaccharides. In: Brett C., Hillman J.R. (Eds), *Biochemistry of plant cell walls*. Cambridge University Press, Cambridge, UK, pp 259–268.

Reid J.S.G., Bewley J.D. (1979) A dual role for the endosperm and its galactomannan reserves in the germinative physiology of fenugreek (*Trigonella foenum-graecum* L.), an endospermic leguminous seed. *Planta*, **147**, 145–150.

Reis D., Vian B., Darzens D., Roland J.C. (1987) Sequential patterns of intramural digestion of galactoxyloglucan in tamarind seedlings. *Planta*, **170**, 60–73.

Rolston M.P. (1978) Water impermeable seed dormancy. *Botanical Review*, **44**, 365–396.

Saeman J.F., Buhl J.L., Harris E.E. (1945) Quantitative saccharification of wood and cellulose. *Industrial Engineer and Chemical Analyses*, **17**, 35–37.

Sampaio A.B., Holl K.D., Scariot A. (2007) Regeneration of seasonal deciduous forest tree species in long-used pastures in central Brazil. *Biotropica*, **39**, 655–659. https://doi.org/10.1111/j.1744-7429.2007.00295.x

Schulze M., Grogan J., Landis R.M., Vidal E. (2008) How rare is too rare to harvest? Management challenges posed by timber species occurring at low densities in the Brazilian Amazon. *Forest Ecology and Management*, **256**, 1443–1457.

Souza F.M., Batista J.L.F. (2004) Restoration of seasonal semideciduous forests in Brazil: influence of age and restoration design on forest structure. *Forest Ecology and Management*, **191**, 185–200. https://doi.org/10.1016/j.foreco.2003.12.006

Souza R.P., Válio I.F.M. (2001) Seed size, seed germination, and seedling survival of Brazilian tropical tree species differing in successional status. *Biotropica*, **33**, 447–457.

Stubblebine W., Langenheim J.H., Lincoln D. (1978) Vegetative response to photoperiod in the tropical leguminous tree *Hymenaea courbaril* L. *Biotropica*, **10**, 18–29.

Tiné M.A.S., Cortelazzo A.L., Buckeridge M.S. (2000a) Xyloglucan mobilisation in cotyledons of developing plantlets of *Hymenaea courbaril* L. (Leguminosae-Caesalpinoideae). *Plant Science*, **154**, 117–126.

Tiné M.A.S., Cortelazzo A.L., Buckeridge M.S. (2000b) Occurrence of xyloglucan containing protuberances in the storage cell walls of cotyledons of *Hymenaea courbaril* L. *Revista Brasileira de Botânica*, **23**, 413–417.

Tiné M.A.S., Lima D.U., Buckeridge M.S. (2003) Galactose branching modulates the action of cellulase on seed storage xyloglucans. *Carbohydrate Polymers*, **52**, 135–141.

Tiné M.A.S., Silva C.O., Lima D.U., Carpita N.C., Buckeridge M.S. (2006) Fine structure of a mixed-oligomer storage xyloglucan from seeds of *Hymenaea courbaril*. *Carbohydrate Polymers*, **66**, 444–454.

Tran V.N., Cavanagh A.K. (1984) Structural aspects of dormancy. In: Murray D.R. (Ed), *Seed physiology, Vol. 2. Germination and reserve mobilization*. Academic Press, Sydney, Australia, pp 1–44.

Ulvskov P., Wium H., Bruce D., Jørgensen B., Qvist K.B., Skjøt M., Hepworth D., Borkhardt B., Sørensen S.O. (2005) Biophysical consequences of remodeling the neutral side chains of rhamnogalacturnonan I in tubers of transgenic potatoes. *Planta*, **220**, 609–620.

Van Acker R., Vanholme R., Storme V., Mortimer J.C., Dupree P., Boerjan W. (2013) Lignin biosynthesis perturbations affect secondary cell wall composition and saccharification yield in *Arabidopsis thaliana*. *Biotechnology for Biofuels*, **6**, 46. https://doi.org/10.1186/1754-6834-6-46

van Dongen J.T., Ammerlaan A.M., Wouterlood M., Van Aelst A.C., Borstlap A.C. (2003) Structure of the developing pea seed coat and the post-phloem transport pathway of nutrients. *Annals of Botany*, **91**, 729–737. https://doi.org/10.1093/aob/mcg066

Verdier J., Dessaint F., Schneider C., Abirached-Darmency M. (2012) A combined histology and transcriptome analysis unravels novel questions on *Medicago truncatula* seed coat. *Journal of Experimental Botany*, **64**, 459–470. https://doi.org/10.1093/jxb/ers304

Vertucci C.W., Leopold A.C. (1983) Dynamics of imbibition of soybean embryos. *Plant Physiology*, **72**, 190–193.

Vertucci C.W., Leopold A.C. (1987) Water binding in legume seeds. *Plant Physiology*, **85**, 224–231.

Vincken J.P., Schols H.A., Oomen R.J.F.J., McCann M.C., Ulvskov P., Voragen A.G.J., Visser R.G.F. (2003) If homogalacturonan were a side-chain of rhamnogalacturonan I: implications for cell wall architecture. *Plant Physiology*, **132**, 1781–1789.

Volodymyr R., Ljudmilla B. (2014) Physical, metabolic, and developmental functions of the seed coat. *Frontiers in Plant Science*, **5**, 510. https://doi.org/10.3389/fpls.2014.00510

Waggoner P.E., Parlange J. (1976) Water uptake and water diffusivity of seeds. *Plant Physiology*, **57**, 153–156.

Whitney S.E.C., Brigham J.E., Darke A.H., Reid J.S.G., Gidley M.J. (1995) *In vitro* assembly of cellulose/xyloglucan networks – Ultrastructural and molecular aspects. *The Plant Journal*, **8**, 491–504.

Whitney S.E.C., Brigham J.E., Darke A.H., Reid J.S.G., Gidley M.J. (1998) Structural aspects of the interaction of mannan-based polysaccharides with bacterial cellulose. *Carbohydrate Research*, **307**, 299–309.

Xue F.C., Chandra R., Berleth T., Beatson R.P. (2008) Rapid, microscale, acetyl bromide-based method for high-throughput determination of lignin content in *Arabidopsis thaliana*. *Journal of Agricultural and Food Chemistry*, **56**, 6825–6834. https://doi.org/10.1021/jf800775f

Yang X., Baskin J.M., Baskin C.C., Huang Z. (2012) More than just a coating: ecological importance, taxonomic occurrence and phylogenetic relationships of seed coat mucilage. *Perspectives in Plant Ecology, Evolution and Systematics*, **14**, 434–442.

York W.S., van Halbeek H., Darvill A.G., Albersheim P. (1990) Structural analysis of xyloglucan oligosaccharides by ^{1}H-NMR spectroscopy and fast-atom-bombardment mass spectrometry. *Carbohydrate Research*, **200**, 9–31.